First publ. in: Journal of colloid and interface science ; 355 (2011), 1. - S. 115-123

Towards nanoscale composite particles of dual complexity

Claudia Simone Wagner [a], Samuel Shehata [a], Katja Henzler [b], Jiayin Yuan [c], Alexander Wittemann [a,*]

[a] Physikalische Chemie I, Universität Bayreuth, Universitätsstr. 30, 95440 Bayreuth, Germany
[b] Institute for Soft Matter and Functional Materials, Helmholtz-Zentrum Berlin, Hahn-Meitner-Platz 1, 14109 Berlin, Germany
[c] Max Planck Institute for Colloids and Interfaces, Am Mühlenberg 1, 14476 Potsdam, Germany

The fabrication of heteroaggregates comprising inorganic and organic nanoparticles of different sizes is reported. Control over the assembly of nanoscale functional building units is of great significance to many practical applications. Joining together different spherical nanoparticles in a defined manner allows control over the shape of the composites. If two types of constituents are chosen that differ in size, the surfaces of the composites exhibit two specific radii of curvature, yielding aggregates of dual surface roughness. Moreover, if the constituents consist of different materials, the resulting heteroaggregates feature both compositional and interfacial anisotropy, offering unprecedented perspectives for custom-tailored colloids. This study describes a two-step approach towards such designer particles. At first, amine-modified polystyrene particles with 154 nm diameter were assembled into clusters of well-defined configurations. Onto these, oppositely charged inorganic particles with diameters of only a few nanometres were deposited by direct uptake from solution, resulting in numerous functional entities all over the surface of the polymer clusters. Despite the fact that oppositely charged constituents are brought together, charge reversal by uptake of nanoparticles allows for stable suspensions of heterocomposites. Hence, the possibility to assemble particles into nanoscale heterocomposites with full control over shape, composition, and surface roughness is demonstrated.

1. Introduction

The design of particles that combine well-defined geometries with a substantial complexity has emerged to a current frontier in colloid and particle research [1,2]. If this complexity encompasses both compositional and interfacial anisotropy, such tailor-made objects may open unprecedented opportunities that cannot be provided by simple mixtures of their individual constituents [3,4]. In order to express the enthusiasm associated with such designer particles, terms like "colloidal molecules" [5–7] or "patchy particles" [3] were established. Unlike isotropic objects, such particles having at least one patch on their surface can undergo directed interactions like organic molecules [5,8]. This, in turn, allows control on their assembly into novel hierarchically organized architectures [9–11]. In this regard, there is a broad similarity to pathways created by mother nature to assemble proteins [12]. The surface of proteins is subdivided into distinct patches which are essential for the formation of fibrils, spherulites, capsids, and fractal clusters [13].

Mimicking this approach, much work was devoted to synthetic colloidal particles bearing single or multiple patches on their surface. This can be accomplished through surface modification of isotropic colloids [5,14,15]. If the particles are made up of different components, they have patterned surfaces as well as anisotropic compositions. Such hybrids can thus unite individual properties of their different components in an advantageous way. Janus particles consisting of two different halves are typical representatives of hybrids [16,17].

Among hybrid particles, "raspberry particles", i.e. colloids bearing smaller particles on their surface, have emerged into a promising class in itself in recent years. Once deposited to a surface, superhydrophobic films can be formed [18–20]. The dual-size surface roughness of such coatings mimics water-repellent self-cleaning plant leaves. Synthetic strategies towards raspberry particles include: (1) covalent grafting of small particles to larger ones [19], (2) miniemulsion [21], emulsion [22] or dispersion polymerization [23] using nanoparticles as stabilizers, and (3) the generation of nanoparticles on the surface of colloidal carriers [18,20,24–26]. A straightforward route is the direct adsorption of oppositely charged particles on larger colloids [27–31].

All these studies have in common that they are based on spherical colloids with small entities on their surface. Here we present a novel type of raspberry-like particles, which are based on nanoscopic clusters of polystyrene (PS) spheres bearing inorganic nanoparticles (NPs) on their surface (Fig. 1). These complex colloids could further extend the potential use of hybrid particles having

* Corresponding author. Fax: +49 (0) 921 55 2780.
E-mail address: Alexander.Wittemann@uni-bayreuth.de (A. Wittemann).

doi:10.1016/j.jcis.2010.12.017

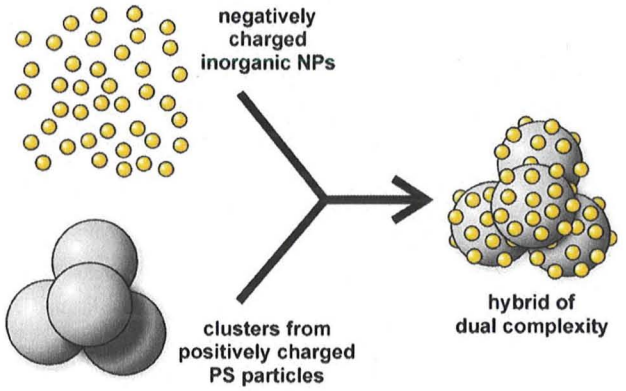

Fig. 1. Schematic representation of the preparation of hybrids with dual surface roughness: A suspension of submicron-sized clusters of amine-modified polystyrene (PS) particles is added to a suspension of oppositely charged inorganic nanoparticles (NPs). The direct deposition of the NPs onto well-defined pre-formed clusters leads to assemblies with diameters below 400 nm that combine patterned surfaces with compositional anisotropy.

well-defined shapes. They provide dual complexity in a double sense because they exhibit two different radii of curvature as well as compositional and interfacial anisotropy.

2. Experimental

2.1. Materials

2.1.1. Amino-functionalized polystyrene particles

A detailed description of the preparation of the cross-linked PS particles bearing amino moieties on their surface is given in Ref. [32]. The spherical particles with an average diameter of 154 nm can be regarded as monodisperse (Fig. 2a) and are thus ideal building units for clusters of well-defined geometries. The high density of positive surface charges is corroborated by the value of the zeta potential (Table 1).

2.1.2. Silica nanoparticles

Commercially available 20.7 nm sized anionic silica NPs (Ludox HS, Aldrich, Fig. 2b) were purified by dialysis against deionized water (Milli-Q, Millipore) until the conductivity of the surrounding water was consistent to that of pure water. All important parameters of the particles are gathered in Table 1.

2.1.3. Gold nanoparticles

Negatively charged gold particles of 23.0 nm in diameter (Fig. 2c) were prepared by precipitation of $HAuCl_4$ in the presence of trisodium citrate dihydrate along the lines given in Ref. [33]. In a typical batch, a solution of 84.5 mg $HAuCl_4$ in 150 g deionized water was brought to boil under permanent stirring. 19.8 ml of 0.034 M trisodium citrate dihydrate were added. An immediate colour change from bright yellow to dark red was observed. The mixture was heated under reflux for another 15 min. Then the dispersion was cooled to room temperature and purified by exhaustive dialysis against deionzed water. Decisive data on the gold NPs is given in Table 1.

2.1.4. Maghemite nanoparticles

Negatively charged maghemite NPs were synthesized following a protocol given in Ref. [34]. At first, a stock solution of 128.5 mmol NaOH dissolved in 51 ml diethylene glycol (Sigma–Aldrich) was heated up to 120 °C for one hour under continuous nitrogen flow. This solution was cooled down to 70 °C and stored at this temperature until use. In a separate reaction vessel, 32 mmol poly(acrylic acid) (Aldrich, $M_w = 1800\ g\ mol^{-1}$), 16 mmol anhydrous $FeCl_3$ (Sigma–Aldrich) and 120 ml diethylene glycol were heated carefully to 220 °C under a nitrogen atmosphere and vigorous stirring. Right after rapid addition of 32 ml stock solution, the mixture turned dark black. The reaction mixture was further refluxed for 45 min to yield NPs. After cooling down to room temperature, the NPs were transferred to water by exhaustive dialysis.

Because of their small dimensions of 7 nm in diameter (Fig. 2d and Table 1), the quasi-spherical NPs might be considered as a state of matter between large atomic clusters and crystalline particles. Mössbauer spectra clearly indicated that the particles consist predominantly of maghemite, whereas the particles were regarded as magnetite particles in the original paper [34]. Surface oxidation of magnetite [35] or slight variations in experimental conditions [36] could result in partial or complete conversion into maghemite, which might explain the different findings.

2.2. Nanoparticle adsorption

Small amounts of suspensions of either PS particles or clusters from PS particles were added dropwise under vigorous stirring into aliquouts of suspensions of the inorganic NPs using a syringe pump (kdScientific KDS 100). Detailed amounts are given in Table 2. The mixtures were kept at 25 °C and equilibrated for at least 24 h. For removal of unbound NPs, the samples were placed into ultrafiltration cells (Whatman cellulose nitrate membrane, pore sizes 100 nm) and flushed extensively against deionized water. The progress of the ultrafiltration was monitored by the conductivity of the eluate.

2.3. Methods

The morphologies of particles and particle assemblies were analyzed by field emission scanning electron microscopy (FESEM) on a Zeiss LEO 1530 Gemini microscope equipped with a field emission cathode operating at 3 kV. Specimen preparation was accomplished as follows: silicon wafers (CrysTec) were cleaned using standard RCA-1 at 75 °C with a 5:1:1 mixture of water, 30% H_2O_2 solution, and 25% NH_3 solution. Thereafter the wafers were rinsed in water, blow-dried with N_2, treated with O_2 plasma (Harrick Plasma PDC-32G) during 20 min, and transferred into a $1\ g\ L^{-1}$ aqueous solution of poly(ethylene imine). This treatment results in a thin hydrophilic cationic surface layer providing deposition of the assemblies apart from each other. One drop of each hybrid suspension was placed onto the wafers. After 2 min, the drops were gently swept away by touching the edge of the wafers with filter paper. Specimens were coated twice with platinum layers of 1 nm thickness using a sputter coater (Cressington 208HR) to make the specimen conductive.

Transmission electron micrographs (TEM) were taken on a Zeiss EM922 EFTEM. The average size and polydispersity of the particles were determined by counting at least 500 individual particles.

Electrophoretic mobilities u of the polymer particles and the inorganic NPs were measured on a Malvern Zetasizer Nano ZS. The ionic strength was properly fixed by addition of NaCl to 10^{-4} M. Given this condition, the radii of the NPs a are smaller than the Debye length κ^{-1}, i.e. $\kappa a < 1$. However, in the case of the PS particles, both quantities, a and κ^{-1}, are of the same magnitude. To ensure validity for all values of κa, the mobilities were converted into zeta potentials ζ using the approximation of Henry's formula by Ohshima [37].

The electrophoretic mobilities of the composite particles as the function of the dose of NPs were measured in conjunction with a Malvern MPT2 Autotitrator. Minute amounts of a 0.45 wt.% silica NPs suspension were titrated into 10 g 0.20 wt.% suspensions of

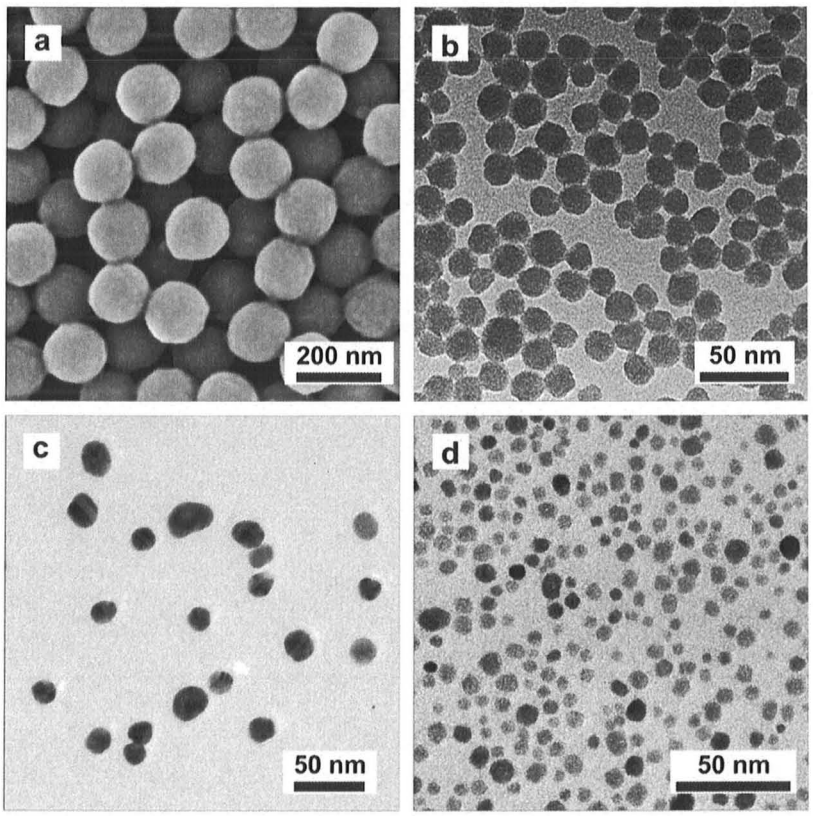

Fig. 2. Micrographs of the particles used in this study: (a) FESEM micrograph of amine-modified PS particles, (b–d) TEM micrographs of silica NPs (b), gold NPs (c), and maghemite NPs (d). All particles exhibit narrow-dispersed size distributions, which makes them ideal building blocks for hierarchical organized materials.

Table 1
Characterization of the constituent particles of the nanocomposites.

Particles	d_n[a] (nm)	d_w[b] (nm)	PDI[c]	u[d] ($m^2 V^{-1} s^{-1}$)	ζ[e] (mV)	ρ[f] ($g\ cm^{-3}$)
PS	154	155	1.004	$+5.1 \times 10^{8}$	+92	1.054
Silica	20.7	20.9	1.01	-3.9×10^{8}	−74	2.20
Gold	23.0	24.2	1.06	-3.0×10^{8}	−58	19.30
Maghemite	7.1	7.7	1.07	-4.0×10^{8}	−77	4.9

[a] Number-average diameter as determined from TEM micrographs.
[b] Weight-average diameter as determined from TEM micrographs.
[c] Polydispersity index given as d_w/d_n.
[d] Electrophoretic mobility.
[e] Zeta potential derived from the mobility as described in Ref. [37].
[f] Particle density.

Table 2
Specifications of the preparation of heteroaggregates.

Experiment	m_{PS}[a] (mg)	N_{PS}[b]	m_{NPs}[c] (mg)	N_{NPs}[d]	N_{NPs}/N_{PS}
Silica NPs on PS spheres	40.0	1.99×10^{13}	1.4–44.7	1.38×10^{14}–4.40×10^{15}	7–222
Silica NPs on PS clusters	10.0	4.96×10^{12}	10.2	1.00×10^{15}	202
Gold NPs on PS clusters	0.3	1.49×10^{11}	7.3	5.98×10^{13}	401
Maghemite NPs on PS clusters	10.0	4.96×10^{12}	8.5	9.10×10^{15}	1834

In each experiment, the total volume after joining the PS and NPs suspensions was fixed to 20 ml.
[a] Mass of PS particles.
[b] Number of PS particles.
[c] Mass of NPs.
[d] Number of NPs.

PS particles, so that the NPs dose gradually increased by 0.01 wt.%. Two measurements were taken 30 s after each titration step to ensure equilibration.

Thermogravimetric analyses (TGA) were performed on a Mettler TGA/SDTA 85. Small amounts of the suspensions of composite particles were freeze-dried (Christ freeze dryer Alpha) and

heated from 30 °C to 800 °C, with a rate of 10 K min^{-1} in an air flow. The samples were kept at 800 °C for further 360 min. The ratio of inorganic NPs per PS particle was calculated from the total mass loss of the sample.

Isothermal titration calorimetry (ITC) experiments were performed on a VP-ITC from Microcal. Aqueous suspensions of silica NPs and PS particles were exhaustively dialyzed against 0.1 mM NaCl solution to adjust the ionic strength. After degassing, silica NPs (1.08 wt.%) were titrated into a 0.22 wt.% suspension of PS particles at 25 °C. In total, 29 injections spaced by 210 s were made, each with a volume of 10 µl. The increase of the volume was included in the data analysis. The time for acquisition between two data points was set to 2 s. Given the densities of polystyrene and silica NPs (Table 1), the concentrations by weight can be converted into the number of moles of particles. Data were fitted with the software Origin (Microcal) using a simple model based on a single set of individual independent binding sites [38]. The stoichiometry N, the binding constant K, and the adsorption enthalpy ΔH are variable parameters of this binding model. The entropy of the adsorption ΔS was calculated from ΔH and K using the following thermodynamic relationship:

$$\Delta S = \Delta H/T + R\ln K$$

where T denotes the absolute temperature and R is the ideal gas constant.

3. Results and discussions

Cross-linked PS latex particles with diameters of 154 nm bearing positively charged moieties on their surface were combined into clusters of a small number of constituent spheres according to the lines given in Refs. [32,39]. The cluster preparation is based on the agglomeration of the constituent particles while adsorbed onto the surface of emulsion droplets. In contrast to our earlier studies, emulsification was performed without any surfactant to make sure that the surfaces of the resulting assemblies were not shielded by a steric layer of surfactant.

Emulsions solely stabilized by small solid particles are often referred as Pickering emulsions [40]. Remarkably, we found that already a limited number of less than 12 PS particles provided efficient short-term stabilization. In addition to the stabilizing effect, the confinement to the droplets can be used as a template for the particle assembly [41,42]. The size distribution of the templating emulsion droplets was controlled by ultrasound [39]. Evaporation of the dispersed phase creates capillary forces which pack the particles together into clusters that exhibit well-defined configurations, such as particle doublets, triplets, tetrahedrons, triangular dipyramids, and octahedrons, among others [32]. Because the dispersed phase presents a solvent for polystyrene, the cluster constituents are swollen during the assembly. For this reason, the resulting assemblies are very robust. It turned out that even repeated sonication with powerful ultrasound did not break the clusters apart. Because of their shape anisotropy, the dynamics, especially the rotational diffusion, of these complex colloids with dimensions of less than 400 nm is significantly different from spherical particles [43].

The next higher level of hierarchy can be achieved by placing a second type of particles with smaller dimensions onto the surface of the pre-formed polymer assemblies. For this purpose, the clusters of positively charged polymer particles were added into a suspension of negatively charged inorganic NPs. The direct adsorption of the oppositely charged NPs from solution resulted in the formation of complex hybrid particles with well-defined shapes, given appropriate experimental conditions (Fig. 1), which will be discussed below.

It is clear that the deposition of oppositely charged particles results in oppositely charged entities on the larger colloidal support. Hence, attractive patch-patch interactions might arise from the adsorption, which could trigger flocculation of the suspensions. The phenomenon behind this, namely the heterocoagulation of binary mixtures of oppositely charged colloids, was extensively studied in recent decades [44–46]. In order to obtain stable suspensions of well-defined hybrid colloids instead of macroscopic flocs, it is thus crucial to detect appropriate experimental parameters for the adsorption process. For this reason, prior to experiments on polymer clusters, adsorption studies were performed on the constituents of the clusters, i.e. polymer spheres of 154 nm in diameter.

3.1. Adsorption of silica NPs onto polymer spheres

Defined amounts of silica NPs were gently added into aliquots of a suspension of PS particles under permanent stirring. The ratio of silica NPs to PS particles was ranging from 14 to 215 in these experiments. Interestingly, the mixtures of the oppositely charged colloids formed stable suspensions at low as well as at high ratios of added NPs per PS particle, whereas immediate flocculation was observed in between (Fig. 3a).

To get more insight into this, the amount of bound NPs was determined after removal of unbound NPs by TGA analysis of the composites. As long as not more than approx. 82 silica NPs were added per PS particle, the vast majority of NPs was bound. It is evident that the high affinity of the NPs to the PS particles is explained by the strong electrostatic attraction among the oppositely charged particles. Further addition of NPs did not increase the degree of adsorption anymore (Fig. 3b). FESEM micrographs showed that the state of maximum loading is characterized by a quite even distribution of the NPs over the surface of the PS spheres (Fig. 3c). Given the radii of both types of particles, 32% of the total PS surface is covered with NPs at maximum loading. This is in accord with the FESEM micrographs which indicate individual NPs or groups of few NPs on the PS surface that are spatially separated from each other (Fig. 3c). Obviously, the number of binding sites is limited by the net charge of the support and electrostatic double layer repulsions among the NPs. Because the experiments were performed in pure water, the adsorbed NPs are completely located within the electrostatic double layer of the large particles. The NPs can be thus regarded as multivalent counterions of the PS particles.

For this reason, they should be mobile along the surface of the larger colloids which would explain the pretty even distribution of the NPs on the PS surface. It has to be noted that double layer repulsions among NPs are less strong than in the bulk if located within the double layer of larger colloids. This could explain the existence of groups of NPs on the PS surface. Similar observations were made by Vincent and co-workers [45].

The electrophoretic mobilities revealed a reversal from net positive to net negative charge during the course of adsorption (Fig. 3b). Below the isoelectric point (IEP), i.e. at low doses of NPs, the mixture of the two colloidal components forms a stable suspension because the positive charge of the PS particles is only partially compensated by the NPs. As the dose of NPs increases, the net charge of the composites decreases, and so does the electrostatic repulsion among the composites. Near the IEP, which corresponds to 70 NPs per PS particle, the electrostatic repulsion is insufficient to prevail over attractions among oppositely charged parts on the composite particles and van der Waals attractions. For this reason, large flocs are formed which then precipitate. Because the IEP is below the point where maximum coverage is attained, there are still uncovered areas on the PS surface. Above the IEP, further uptake of NPs overcompensates the positive net charge of the PS particles and thus restabilizes the suspension.

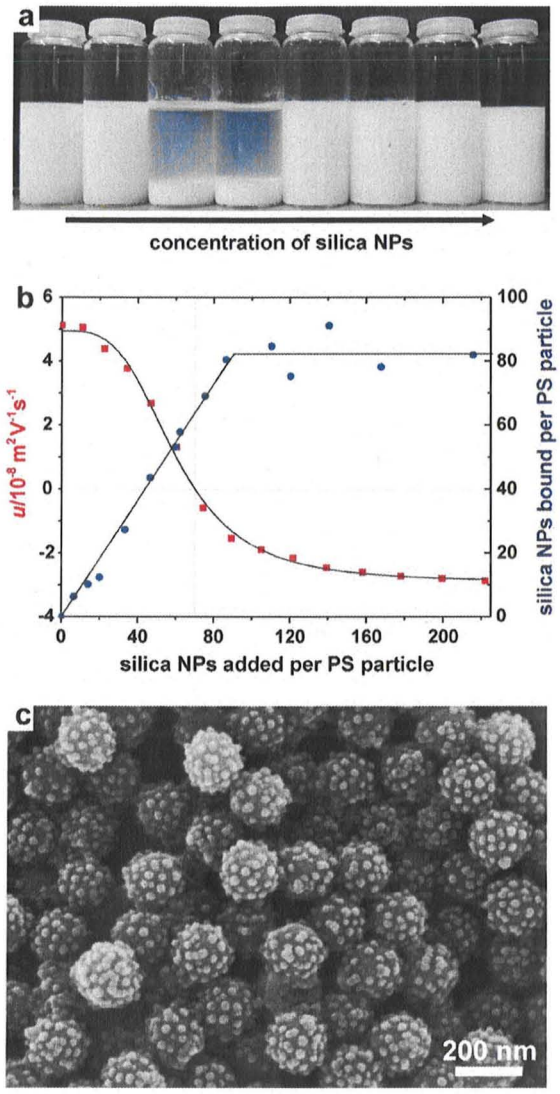

Fig. 3. Adsorption of silica NPs on individual PS particles of opposite charge: (a) series of experiments at varying dose of NPs (14, 38, 62, 86, 110, 120, 168, 215 NPs per PS particle were added from left to right). (b) Progression of the average amount of NPs bound per PS particle and the electrophoretic mobility of the composites with the dose of NPs. (c) FESEM micrographs reveal "raspberry type" morphologies of the composite particles at maximum loading with NPs.

Indeed the layer of negatively charged NPs provided an excellent long-term stability of the suspension of composite particles. Our findings with NPs are in accord with earlier flocculation studies on binary mixtures of oppositely charged PS latexes [45], and electrophoretic measurements on the adsorption of dendrimers on oppositely charged microspheres [47].

A point to be made in regard to the adsorption at moderate doses of NPs is that FESEM micrographs showed marked loading with NPs on specific PS particles, while others were hardly charged. The reason to this is not clear. Maybe subtle mixing effects arise during composite formation. From this disproportionation in NPs loading attractive interactions among oppositely charged surface areas of the composites may arise, which favour flocculation at moderate loading with NPs.

ITC was used to determine the thermodynamics and stoichiometry of the interaction among the PS particles and the NPs. The NPs were titrated in multiple injections into the sample cell containing a suspension of PS particles. An ITC experiment measures the difference in heat which has to be added to the sample and reference cells to keep them both at the same temperature. For an exothermic reaction in the sample, less heat is required to heat up the sample cell and thus negative signals are recorded. It is thus obvious from the ITC data shown in Fig. 4 that the uptake of the NPs is exothermic. Moreover, because the concentrations of NPs and PS particles are known, the ITC data provides information on the number of NPs bound per PS particle, i.e. the stoichiometry of the adsorption process, and the absolute value of the change in enthalpy ΔH. The ITC data could be fitted assuming a single set of individual binding sites for the adsorption (Fig. 4). This implies that the uptake of a NP is independent on the occupancy of neighbouring sites. The stoichiometry shows that 68 ± 3 NPs are bound per PS particle on average. This value is lower than the one obtained from the TGA experiment. The deviation might come from the fact the ionic strength was fixed to 0.1 mM in the ITC study to exclude enthalpy changes due to changes in the salinity, whereas all other experiments were carried out in deionized water. This results in partial screening of the electrostatic attraction among NPs and PS particles in the ITC experiment.

An enthalpy change ΔH of -9800 ± 700 kJ mol^{-1} and an equilibrium association constant K of $30 \times 10^6 \pm 5 \times 10^6$ M^{-1} was associated with the uptake of the NPs. The entropy change ΔS calculated from these two quantities is -33 ± 2 kJ mol^{-1}K^{-1}. Hence, the change in entropy must be governed by the loss of translational entropy of the NPs because other phenomena such as the release of counterions or water molecules from the surface of the particles would increase the entropy. Interestingly, negative values for ΔS were also found for the binding of the protein serum albumin to PS particles [48].

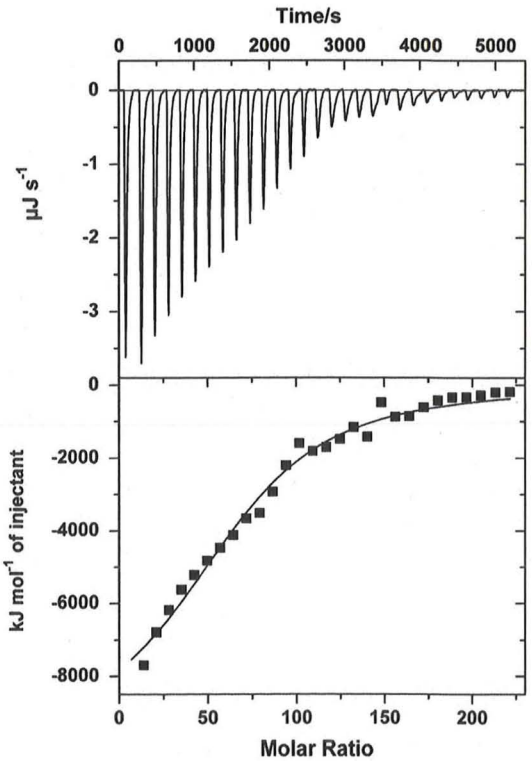

Fig. 4. ITC raw data (top) and integrated heats (below) of a titration of cationic PS particles with negatively charged silica NPs in 0.1 mM NaCl solution at 25 °C. It can be clearly seen that the adsorption of the NPs onto the surface of the oppositely charged colloids is exothermic at each stage.

3.2. Hybrids with complex shapes

The results of the previous section have shown how experimental parameters must be chosen in order to yield stable suspensions of composite particles. Based on these results we replaced the simple PS particles by the above-mentioned robust clusters of PS particles aiming at hierarchically organized particle assemblies that exhibit a high level of complexity. Because the pre-assembly of the PS particles is based on emulsion droplets bearing statistically distributed particles, different species with well-defined complex shapes are accessible (left column in Fig. 5). The mixture of different species made from up to 12 constituents can be separated into fractions of uniform clusters by density gradient centrifugation [39]. This offers the possibility to prepare uniform colloidal supports for the NPs exhibiting different defined shapes, which in turn provides full control over composition and shape of the resulting binary heteroaggregates (Fig. 5). In the following, the deposition of NPs was solely performed on mixtures of PS clusters because the present study is devoted to a proof of concept.

At first, the deposition of silica NPs onto the PS clusters was studied. For this purpose aliquots of a suspension of PS clusters were slowly added to suspensions containing 202 NPs per cluster constituent (Table 2). Hence, the number of NPs was sufficient to ensure charge reversal upon loading of the clusters with NPs. For this reason, the composites exhibited negative net charges and thus formed stable suspensions. The excess of unbound NPs was removed by ultrafiltration of the suspension against deionized water.

Figs. 5 and 6 show synopses of the hybrid clusters that differ in number and configuration of the polymer constituents. The NPs are evenly dispersed all over the surface of the PS clusters. The ordered arrangement of the inorganic entities on the colloidal support is caused by electrostatic repulsions among the NPs within the electric double layer of the PS clusters as already discussed in the previous section.

Yang and co-workers found that the direct combination of particles of two different sizes templated by emulsion droplets resulted in composites with the small spheres located in the

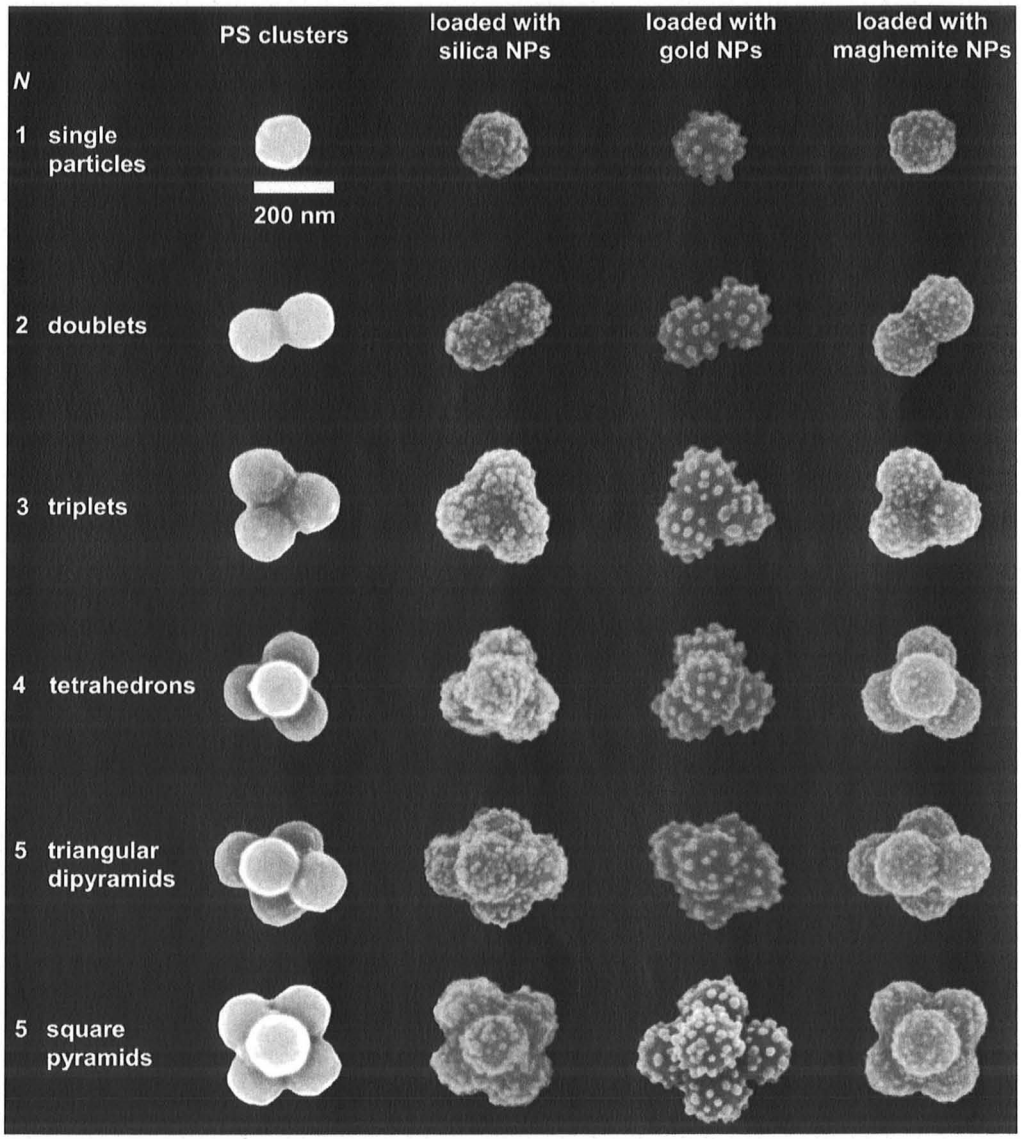

Fig. 5. Synopsis of FESEM micrographs of hybrid nanocomposites produced from different types of inorganic NPs and clusters of amine-modified polymer particles exhibiting well-defined morphologies such as particle doublets, triplets, tetrahedrons, and square dipyramids.

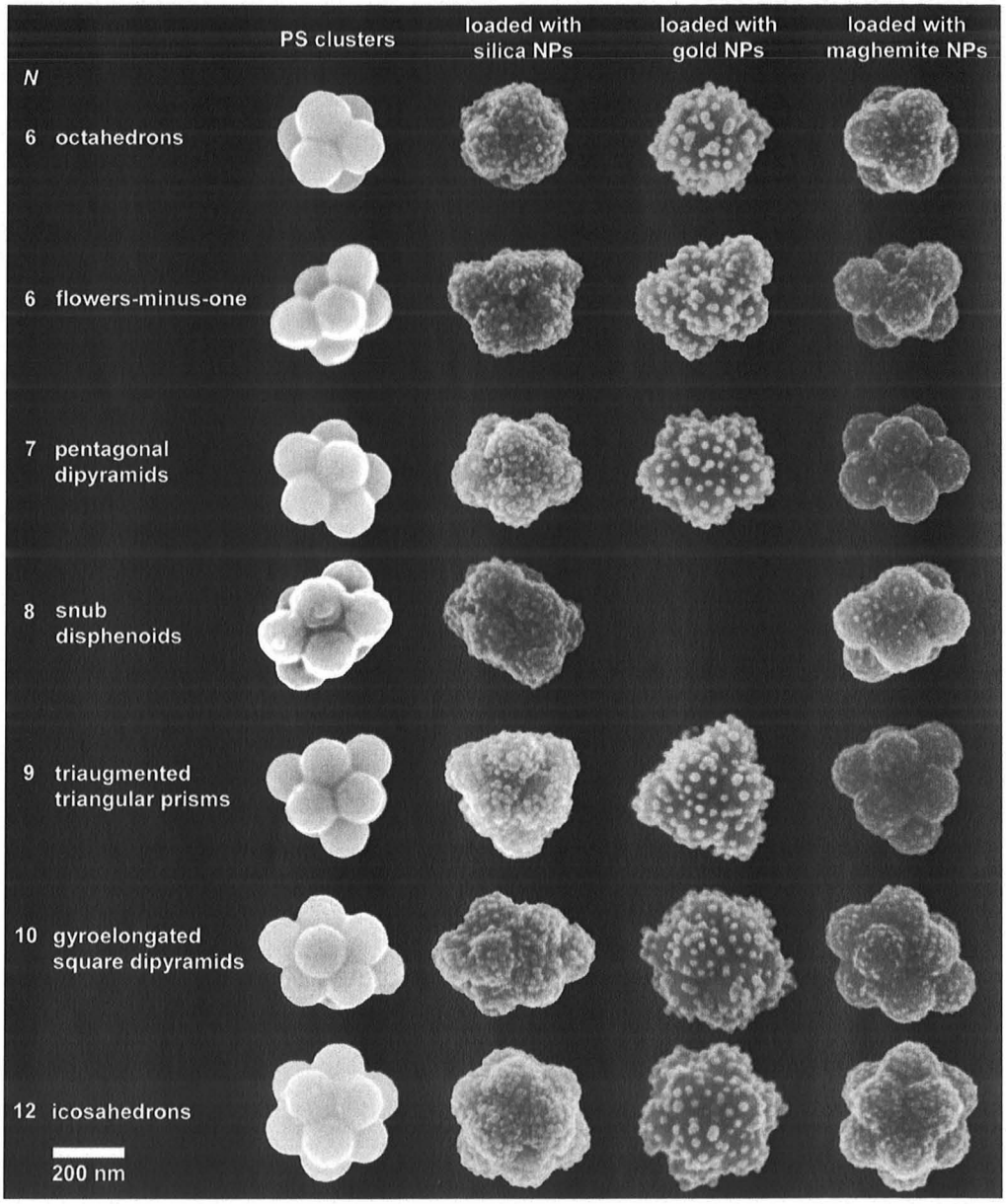

Fig. 6. Silica, gold, and maghemite nanoparticles (NPs) spread over the surface of clusters of six and more amine-modified polystyrene (PS) constituents.

valleys among the bigger particles [49]. Hence, the deposition of NPs onto pre-formed complex colloids as reported in this study allows for a different arrangement of the NPs, which is characterized by spatially separated NPs all over the surface of the composites (Figs. 5 and 6).

The adsorption studies were carried out with gold and maghemite NPs as well. Because these two types of NPs differ in their chemical nature, size and surface charge from the silica NPs, the further experiments contribute to assess the versatility of this route towards complex hybrids. FESEM micrographs of both gold/PS and maghemite/PS hybrid clusters indeed confirm that this approach is a general one which can be applied to a wide variety of particles.

As compared to the silica NPs, the gold NPs were arranged widely isolated on the PS surface. Because the average radii and the zeta potentials of both types of NPs are of the same magnitude (Table 1), the different arrangement might originate from more subtle adhesion effects. However, at maximum loading with NPs, a quite uniform deposition of the NPs over the polymer surface is found in all cases. This together with the small total dimensions of the polymer clusters makes sure that the hybrid structures underlie Brownian motion and form stable suspensions.

The closely but spatially separated arrangement of the gold NPs indicates that the composites should exhibit collective plasmon modes, implying the potential for sensing applications [50]. In fact, keeping gold NPs physically separated but closed spaced has been a challenge in surface-enhanced Raman scattering (SERS) because such an array of NPs can be strongly enhancing [51,52]. It is known that physical separation does not impede gold NPs to interact electromagnetically as long as the spacing among the NPs is small as compared to the wavelength of light [52], which holds for the heterocomposites in this study. Future work will be devoted to such hybrids for SERS.

Applications with regard to ferrofluids [53], i.e. colloidal suspensions of nanoscale particles with either ferro- or ferrimagnetic

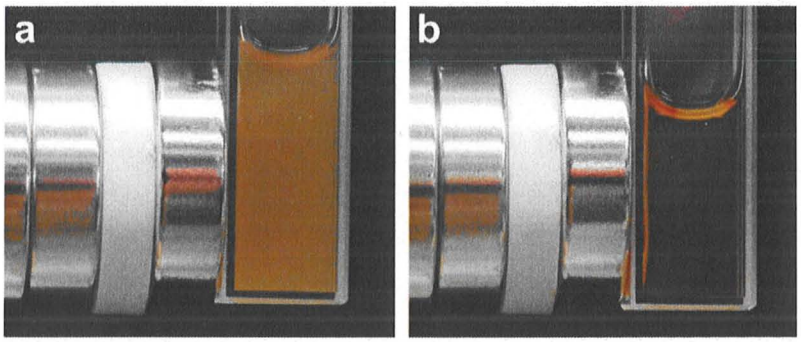

Fig. 7. Magnetic nanocomposites: (a) Deposition of maghemite NPs onto oppositely charged PS clusters results in stable suspensions of complex colloids given appropriate experimental conditions. (b) The ferromagnetic hybrids can be separated by external magnetic fields from the aqueous medium.

properties, can be accomplished by incorporation of NPs that exhibit magnetic properties [28,54]. For this purpose maghemite NPs were used. These particles have smaller dimensions than the silica and gold particles used before. It is known that maghemite particles with dimensions of a few nanometers exhibit superparamagnetic properties [55]. Hence, deposition of maghemite NPs results in small superparamagnetic entities on the surface of the preformed polymer clusters, which allow for separation of the nanocomposites by external magnetic fields (Fig. 7). This opens perspectives for magnetic nanofluids with specific rheological properties and as complex building units for the next level in hierarchy of material design. Promising studies in this direction were already reported based on micron-sized particles with complex shapes [56–58].

4. Conclusion

We have shown that the fabrication of colloidal heteroaggregates from nanoparticles of two different sizes presents a facile but versatile pathway towards a plenitude of functional colloids with tailored geometries of inherent complexity. Control over shape, composition and surface roughness of the heteroaggregates can be managed by tuning the size of the constituents and the aggregation numbers. Both steps in the preparation of heteroaggregates, i.e. formation of clusters and adsorption of NPs, can be accomplished with many other types of particles. This opens perspectives for a vast variety of rationally designed functional colloids which are of fundamental importance to a broad range of applications including sensing, photonic, and electronic devices.

Acknowledgments

We gratefully acknowledge financial support from the Deutsche Forschungsgemeinschaft (DFG) within SFB 840/A3, the Fonds der Chemischen Industrie (FCI), and the Dr. Otto Röhm Gedächtnisstiftung. The help of Christina Löffler during TGA measurements, Yvonne Hertle during TEM measurements, and the support of Christoph Hanske during FESEM specimen preparation is appreciated. We thank Prof. Friedrich Wagner from the Technical University of Munich and Prof. Josef Breu for verifying the chemical modification of the maghemite NPs.

References

[1] S.C. Glotzer, M.J. Solomon, Nat. Mater. 6 (2007) 557.
[2] M. Rycenga, P.H.C. Camargo, Y. Xia, Soft Matter 5 (2009) 1129.
[3] A.B. Pawar, I. Kretzschmar, Macromol. Rapid Commun. 31 (2010) 150.
[4] V. Rastogi, A.A. Garcia, M. Marquez, O.D. Velev, Macromol. Rapid Commun. 31 (2010) 190.
[5] C.E. Snyder, M. Ong, D. Velegol, Soft Matter 5 (2009) 1263.
[6] A. van Blaaderen, Nature 439 (2006) 545.
[7] A. Perro, E. Duguet, O. Lambert, J.-C. Taveau, E. Bourgeat-Lami, S. Ravaine, Angew. Chem., Int. Ed. 48 (2009) 361.
[8] Z. Zhang, S.C. Glotzer, Nano Lett. 4 (2004) 1407.
[9] F. Sciortino, E. Bianchi, J.F. Douglas, P. Tartaglia, J. Chem. Phys. 126 (2007) 194903/1.
[10] A.W. Wilber, J.P.K. Doye, A.A. Louis, E.G. Noya, M.A. Miller, P. Wong, J. Chem. Phys. 127 (2007) 085106/1.
[11] Z. Zhang, A.S. Keys, T. Chen, S.C. Glotzer, Langmuir 21 (2005) 11547.
[12] C.-J. Tsai, J. Zheng, D. Zanuy, N. Haspel, H. Wolfson, C. Aleman, R. Nussinov, Proteins 68 (2007) 1.
[13] E. van der Linden, P. Venema, Curr. Opin. Colloid Interface Sci. 12 (2007) 158.
[14] L. Hong, A. Cacciuto, E. Luijten, S. Granick, Nano Lett. 6 (2006) 2510.
[15] A. Perro, F. Meunier, V. Schmitt, S. Ravaine, Colloids Surf., A 332 (2009) 57.
[16] R. Erhardt, M. Zhang, A. Böker, H. Zettl, C. Abetz, P. Frederik, G. Krausch, V. Abetz, A.H.E. Müller, J. Am. Chem. Soc. 125 (2003) 3260.
[17] N. Glaser, J. Adams Dave, A. Böker, G. Krausch, Langmuir 22 (2006) 5227.
[18] M. D'Acunzi, L. Mammen, M. Singh, X. Deng, M. Roth, G.K. Auernhammer, H.-J. Butt, D. Vollmer, Faraday Discuss. 146 (2010) 35.
[19] W. Ming, D. Wu, R. van Benthem, G. de With, Nano Lett. 5 (2005) 2298.
[20] Z. Qian, Z. Zhang, L. Song, H. Liu, J. Mater. Chem. 19 (2009) 1297.
[21] F. Tiarks, K. Landfester, M. Antonietti, Langmuir 17 (2001) 5775.
[22] A. Schmid, S.P. Armes, C.A.P. Leite, F. Galembeck, Langmuir 25 (2009) 2486.
[23] A. Schmid, S. Fujii, S.P. Armes, C.A.P. Leite, F. Galembeck, H. Minami, N. Saito, M. Okubo, Chem. Mater. 19 (2007) 2435.
[24] W.S. Choi, H.Y. Koo, W.T.S. Huck, J. Mater. Chem. 17 (2007) 4943.
[25] Y. Lu, M. Hoffmann, R.S. Yelamanchili, A. Terrenoire, M. Schrinner, M. Drechsler, M.W. Möller, J. Breu, M. Ballauff, Macromol. Chem. Phys. 210 (2009) 377.
[26] J.-C. Taveau, D. Nguyen, A. Perro, S. Ravaine, E. Duguet, O. Lambert, Soft Matter 4 (2008) 311.
[27] A. Pich, S. Bhattacharya, H.J.P. Adler, Polymer 46 (2005) 1077.
[28] F. Sauzedde, A. Elaissari, C. Pichot, Colloid Polym. Sci. 277 (1999) 846.
[29] G. Li, X. Yang, J. Wang, Colloids Surf., A 322 (2008) 192.
[30] H.-J. Tsai, Y.-L. Lee, Langmuir 23 (2007) 12687.
[31] S. Harley, D.W. Thompson, B. Vincent, Colloids Surf. 62 (1992) 163.
[32] C.S. Wagner, B. Fischer, M. May, A. Wittemann, Colloid Polym. Sci. 288 (2010) 487.
[33] J. Turkevich, P.C. Stevenson, J. Hillier, Discuss. Faraday Soc. 11 (1951) 55.
[34] J. Ge, Y. Hu, M. Biasini, C. Dong, J. Guo, W.P. Beyermann, Y. Yin, Chem. Eur. J. 13 (2007) 7153.
[35] I. Nedkov, T. Merodiiska, L. Slavov, R.E. Vandenberghe, Y. Kusano, J. Takada, J. Magn. Magn. Mater. 300 (2006) 358.
[36] S.Y. An, I.-B. Shim, C.S. Kim, J. Appl. Phys. 97 (2005) 10Q909/1.
[37] H. Ohshima, J. Colloid Interface Sci. 168 (1994) 269.
[38] J.E. Ladbury, B.Z. Chowdhry, Biocalorimetry: Applications of Calorimetry in the Biological Sciences, John Wiley & Sons Ltd., Chichester, 1998.
[39] C.S. Wagner, Y. Lu, A. Wittemann, Langmuir 24 (2008) 12126.
[40] B.P. Binks, T. Horozov, Colloidal Particles at Liquid Interfaces, Cambridge University Press, Cambridge, 2006.
[41] V.N. Manoharan, M.T. Elsesser, D.J. Pine, Science 301 (2003) 483.
[42] O.D. Velev, K. Furusawa, K. Nagayama, Langmuir 12 (1996) 2385.
[43] M. Hoffmann, C.S. Wagner, L. Harnau, A. Wittemann, ACS Nano 3 (2009) 3326.
[44] P. Luckham, B. Vincent, C.A. Hart, T.F. Tadros, Colloids Surf. 1 (1980) 281.
[45] P.F. Luckham, B. Vincent, J. McMahon, T.F. Tadros, Colloids Surf. 6 (1983) 83.
[46] D.J. Voorn, W. Ming, A.M. Van Herk, P.H.H. Bomans, P.M. Frederik, P. Gasemjit, D. Johanssmann, Langmuir 21 (2005) 6950.
[47] W. Lin, P. Galletto, M. Borkovec, Langmuir 20 (2004) 7465.
[48] S. Lindman, I. Lynch, E. Thulin, H. Nilsson, K.A. Dawson, S. Linse, Nano Lett. 7 (2007) 914.
[49] Y.-S. Cho, G.-R. Yi, S.-H. Kim, M.T. Elsesser, D.R. Breed, S.-M. Yang, J. Colloid Interface Sci. 318 (2008) 124.
[50] R.A. Alvarez-Puebla, L.M. Liz-Marzan, Small 6 (2010) 604.

[51] R.A. Alvarez-Puebla, L.M. Liz-Marzan, F.J. Garcia de Abajo, J. Phys. Chem. Lett. 1 (2010) 2428.
[52] K.C. Grabar, R.G. Freeman, M.B. Hommer, M.J. Natan, Anal. Chem. 67 (1995) 735.
[53] A.T. Skjeltorp, S. Clausen, G. Helgesen, J. Magn. Magn. Mater. 226–230 (2001) 534.
[54] F. Caruso, A.S. Susha, M. Giersig, H. Möhwald, Adv. Mater. 11 (1999) 950.
[55] S. Reinicke, S. Döhler, S. Tea, M. Krekhova, R. Messing, A.M. Schmidt, H. Schmalz, Soft Matter 6 (2010) 2760.
[56] S.H. Lee, C.M. Liddell, Small 5 (2009) 1957.
[57] D. Zerrouki, J. Baudry, D. Pine, P. Chaikin, J. Bibette, Nature 455 (2008) 380.
[58] R.M. Erb, H.S. Son, B. Samanta, V.M. Rotello, B.B. Yellen, Nature 457 (2009) 999.